Fluence Dependence of Crystallinity Changes in PEEK Induced by Ultrashort Pulse Laser

Miyu Takahashi¹, Hikaru Yamato¹, Keisuke Takabayashi², Tsubasa Endo², Yohei Kobayashi², Takuro Tomita³, and Makoto Yamaguchi¹

¹Graduate School of Engineering Science, Akita University, Japan

²The Institute for Solid State Physics, University of Tokyo, Japan

³Graduate School of Science and Technology for Innovation, Tokushima University, Japan

*Corresponding author's e-mail:yamaguci@phys.akita-u.ac.jp

In this study, ultrashort pulse laser irradiation was performed on Polyether ether ketone (PEEK) while systematically varying the pulse duration and fluence. Distinct surface morphologies were observed with increasing pulse duration. Under identical pulse durations but varying fluences, laser-irradiated craters exhibiting swelling were observed at fluences near to the threshold peak fluence. To investigate the laser-induced effects around the irradiation region, the crystallinity was evaluated from the intensity ratios of the Raman spectra acquired by line-scan measurements across the irradiation spot using Raman spectroscopy, and changes in crystallinity were observed. It was found that the crystallinity decreased as the measurement point approached the center of the laser-irradiated craters. By converting the measurement positions to the local fluence, it was found that the local fluence for crystallinity change remains nearly the same even as the pulse duration increases. In contrast, the threshold fluence for processing increases as the pulse duration increases.

DOI: 10.2961/ilmn.2025.03.2009

Keywords: ultrashort pulse laser, Raman scattering spectroscopy, crystallinity, Poly Ether Ether Ketone

1. Introduction

Polyether ether ketone (PEEK) is a high-performance thermoplastic polymer with excellent chemical resistance, thermal stability, and mechanical strength. It is widely used as a matrix resin in carbon fiber-reinforced plastics (CFRPs), which have applications in the automotive and aerospace industries. PEEK has also been employed as a biomaterial in the dental and orthopedic fields [1,2]. Laser processing offers non-contact operation and high precision, enabling freeform fabrication and allowing a wide range of tunable parameters. The surface morphology induced by ultrashort pulse laser processing varies significantly depending on the laser wavelength, pulse duration, and fluence.

In ultrashort-pulse laser processing of PEEK, varying the number of pulses and fluence has revealed that cleaner ablation can be achieved at shorter wavelengths than at longer wavelengths [3]. When femtosecond lasers are applied to PEEK with varying degrees of crystallinity under different fluences and pulse numbers, the formation propensity of laser-induced periodic surface structures (LIPSSs) depends on the crystallinity of the sample [4]. Several studies have investigated the effects of laser parameters such as pulse duration, wavelength, and pulse count, and ultrashort-pulse lasers are regarded as promising tools for high-quality PEEK processing [3–7].

Crystallinity, defined as the ratio of the crystalline phase to the amorphous phase in a semicrystalline polymer, is a key indicator of the mechanical properties of thermoplastic polymers. While Wide Angle X-Ray Diffraction (WAXRD) and Fourier Transform Infrared (FTIR) are

commonly used to evaluate crystallinity, micro-Raman spectroscopy enables the quantitative analysis of localized crystallinity owing to its high spatial resolution [8,9]. When PEEK is irradiated with a Continuous Wave (CW) laser, the crystallinity of the irradiated region decreases under conditions of long irradiation time, low feed rate, or high fluence [10–12]. In other words, an increase in laser intensity leads to a decrease in crystallinity. On the other hand, when ultrashort-pulse lasers are applied, both amorphous and semicrystalline samples can undergo cold crystallization, resulting in an increase in crystallinity, as reported in previous studies [4]. Although previous studies have evaluated the crystallinity of laser-processed regions of PEEK, the crystallinity of unprocessed regions has not been reported. Because the laser processing of polymers results in varying surface morphologies depending on the processing parameters, the effects of laser-induced pressure and heat on and around the irradiated spot are also expected to differ [10]. Therefore, understanding the changes in crystallinity induced by ultrashort pulse laser irradiation is essential.

In this study, the effects of pulse duration and fluence on PEEK during ultrashort pulse laser irradiation were investigated. A PEEK film was irradiated with ultrashort pulse lasers of varying pulse durations and fluences, and Raman spectroscopy was conducted around the resulting laser-irradiated craters, which exhibited distinct surface morphologies. The degree of crystallinity was calculated from the intensity ratio of the Raman peaks at 97 cm⁻¹ and 135 cm⁻¹, and the crystallinity at each measurement point was evaluated [13].

2. Material and Methods

A PEEK film (Victrex, 1000-150G; $20 \text{ mm} \times 20 \text{ mm}$; thickness: 150 µm) with a crystallinity of 21% was used as the sample. The surface roughness(R_a), measured with a laser microscope (KEYENCE, VK-X200), was determined to be approximately 0.1 µm. A Yb regenerative amplifier with a central wavelength of 1030 nm was used to irradiate the PEEK film under single-shot conditions. The pulse duration was varied from 300 fs to 10 ps by using the internal pulse compressor of the system. In this study, a bord-type CMOS camera (Camera Module V2; Raspberry Pi Foundation) with a pixel pitch of 2.24 µm was employed. Using this device, the beam profile of the processing laser was spatially measured in situ. The beam profile obtained with the CMOS camera was subjected to a two-dimensional Gaussian fit, from which the beam diameter was determined. The 1/e² intensity diameters of the laser beam were 101 and 108 µm in the x- and y-directions, respectively. Assuming a circular beam profile, the 1/e² intensity radius was approximated using the geometric mean $\sqrt{(xy)} \approx 104$ μm, which resulted in a radius of 52 μm.

The local fluence at each measurement position was calculated and compared with the corresponding Raman spectrum. The local fluence at an arbitrary position was determined using the following equation:

$$F_{(x,y)} = F_0 \times \exp\left[-2\left(\frac{x^2 + y^2}{w^2}\right)\right],$$
 (1)

where F_0 is the peak fluence and w is the beam radius in $1/e^2$.

The laser fluence was varied from 0.2 J/cm² to 4 J/cm² by adjusting the polarization using a half-wave plate and polarizing beam splitter. The pulse duration and laser fluence were systematically varied in 14 steps each, resulting in a total of 196 laser-irradiated craters. After irradiation, the sample was subjected to ultrasonic cleaning to eliminate surface debris.

Micro-Raman spectroscopy (LabRAM HR Evolution, Horiba) was performed along a line passing through the center of each laser-irradiated crater. The excitation wavelength was 1064 nm. The laser beam was focused to a spot size of approximately 1 μm by using a $50\times$ objective lens. The measurement time was 60 s and the signal was integrated three times per point.

3. Result and Discussion

Figure 1 (A)-(F) shows the optical image of laser-irradiated craters. The corresponding peak fluence and pulse duration for each laser-irradiated crater are as follows:(A) 4.0 J/cm², 0.3 ps; (B) 4.0 J/cm², 1.2 ps; (C) 4.0 J/cm², 3.4 ps; (D) 4.0 J/cm², 7.6 ps; (E) 4.0 J/cm², 10 ps; (F) 3.4 J/cm², 10 ps. It is observed that the diameter of the laser-irradiated crater decreases with increasing pulse duration. In Figures 1 (B) to (E), the crater centers appear dark, which can be attributed to surface removal. In contrast, under the condition of the shortest pulse width shown in Figure (A), the surface is less ablated compared to Figures 1 (B) to (E), resulting in a brighter appearance. Furthermore, rim structures are observed on the surface in Figures 1 (B) to (E). Such surface morphologies are often observed in ablation

processes induced by ultrashort pulse lasers and are considered to originate from phase transitions [14].

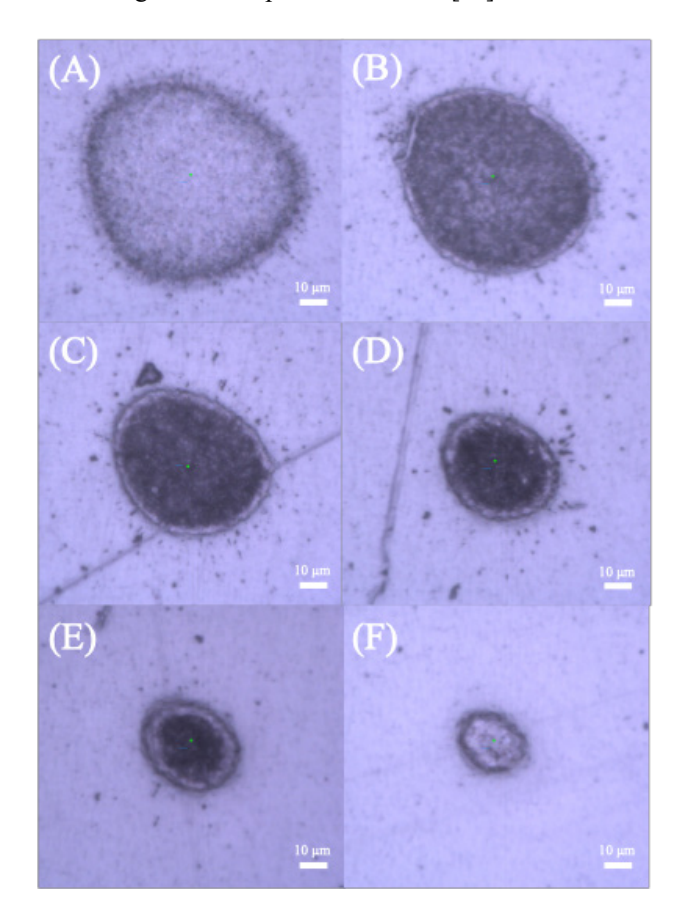


Fig. 1 Optical image of laser-irradiated craters: (A) 4.0 J/cm², 0.3 ps; (B) 4.0 J/cm², 1.2 ps; (C) 4.0 J/cm², 3.4 ps; (D) 4.0 J/cm², 7.6 ps; (E) 4.0 J/cm², 10 ps; (F) 3.4 J/cm², 10 ps.

Figure 2 shows a laser microscope image of the irradiated craters at a fluence of 3.4 J/cm² and a pulse duration of 10 ps. It was observed that the surface of the crater was slightly expanded. Therefore, the surface is considered to appear bright, as observed in Figure 2.

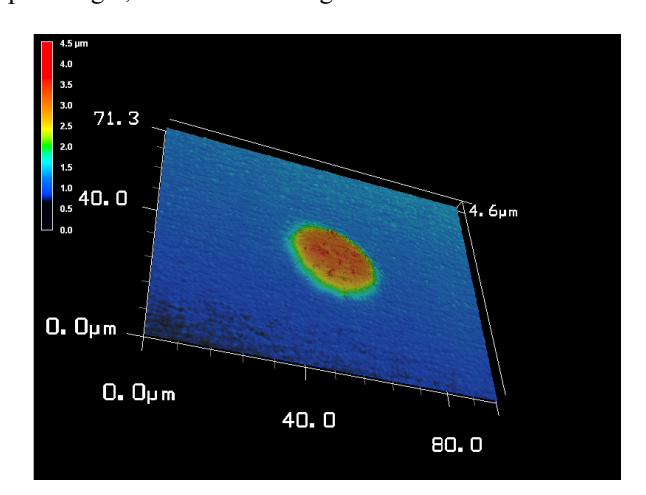


Fig. 2 Laser microscopy image of a laser-irradiated crater of 3.4 J/cm², 10 ps.

Figure 3 shows the Raman measurement positions and the corresponding Raman spectra in the area irradiated with

a laser of 4.0 J/cm^2 and 10 ps. The center of the laser-irradiated crater was defined as $0 \text{ }\mu\text{m}$. Measurement points (a) and (b) in the optical microscope image in Figure 3 correspond to Raman spectra (a) and (b), respectively. It is observed that the point (a) close to the center of the irradiated crater has a lower intensity around 135 cm^{-1} compared to the point (b) far from the center. It was observed that the Raman spectrum changes at each measurement position. A line measurement of the Raman scattering measurement was performed along a line passing through the center of the laser-irradiated crater.

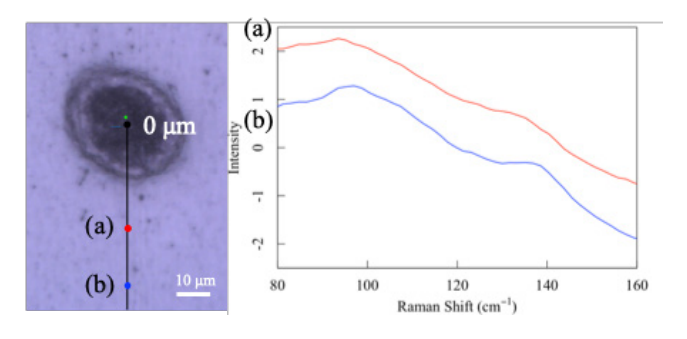


Fig. 3 Raman measurement positions (a) and (b) on the laser-irradiated crater at 4.0 J/cm², 10 ps and their corresponding Raman spectra.

Figure 4 shows an example of the fitting of the Raman spectrum in the non-irradiated region. The Raman scattering spectrum was subjected to Standard Normal Variate (SNV) processing so that the center of intensity was 0 and the variance was 1. The SNV processed spectrum was fitted using two Lorentzian functions with a linear baseline to calculate the crystallinity. The crystallinity was determined from the peak intensity ratio of 97 cm⁻¹ and 135 cm⁻¹ [10]. Line measurements were performed on the irradiated craters shown in Figures 1(A) to (F) as shown in Figure 3, and the crystallinity at each measurement position was calculated.

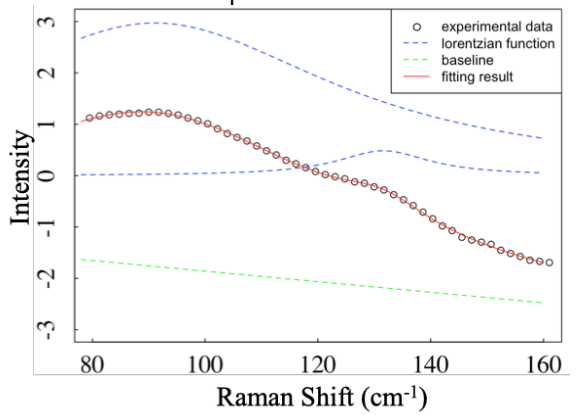


Fig. 4 Fitting results of Raman spectra for the nonirradiated region. The open circles, dashed lines, and solid line correspond to the experimental data, the decomposed components(Lorentzian function and baseline), and the overall fitting result, respectively.

Figure 5 shows the change in crystallinity with distance from the center of each laser-irradiated crater for the following irradiation conditions: (A) 4.0 J/cm², 0.3 ps, (B) 4.0 J/cm², 1.2 ps; (C) 4.0 J/cm², 3.4 ps; (D) 4.0 J/cm², 7.6 ps; (E) 4.0 J/cm², 10 ps; (F) 3.4 J/cm², 10 ps. The dotted lines

indicate the edge of the irradiated crater, i.e., the radius of the laser-irradiated crater, for each irradiation condition. It was observed that the crystallinity decreased with increasing distance from the center of the laser-irradiated crater for all irradiation conditions.

Figure 6 shows the change in crystallinity as a function of local fluence under the following irradiation conditions: (A) 4.0 J/cm², 0.3 ps, (B) 4.0 J/cm², 1.2 ps; (C) 4.0 J/cm², 3.4 ps; (D) 4.0 J/cm², 7.6 ps; (E) 4.0 J/cm², 10 ps; (F) 3.4 J/cm², 10 ps. The measurement positions are converted to local fluence using equation (1). The red dotted lines indicate the positions shown in Fig. 6, converted into local fluence value corresponding to the threshold for processing. It can be seen that the threshold for processing increases with increasing pulse duration. It is noteworthy that the change in crystallinity was observed even below the threshold for processing under all irradiation conditions.

Figure 7 shows a compares the threshold fluence for processing and the threshold fluence for crystallinity change as function of pulse duration. The red filled circle show the threshold fluence for processing from 0.3 ps to 10 ps, while the blue filled circle represent the threshold fluence for crystallinity change taken from Figures 6(A)-(E). Figure 7 shows that the threshold fluence for processing increases with increasing pulse duration, whereas the threshold fluence for crystallinity change remains nearly constant at approximately 1J/cm².

Since the threshold fluence for crystallinity change remains nearly constant, it can be inferred that the region exhibiting crystallinity change does not significantly vary with increasing pulse duration. Since the band gap of PEEK is approximately 3.2 eV, multiphoton absorption is considered to occur during processing at the wavelength of 1030 nm used in this study [3]. It has been reported in previous studies that the crystalline structure of PEEK is destroyed with increasing strain under tensile testing [15]. In the present study as well, since no surface melting or significant morphological changes were observed under optical microscopy, it is considered that PEEK is heated during ultrashort pulse laser irradiation, generating stress, which in turn decreases its crystallinity.

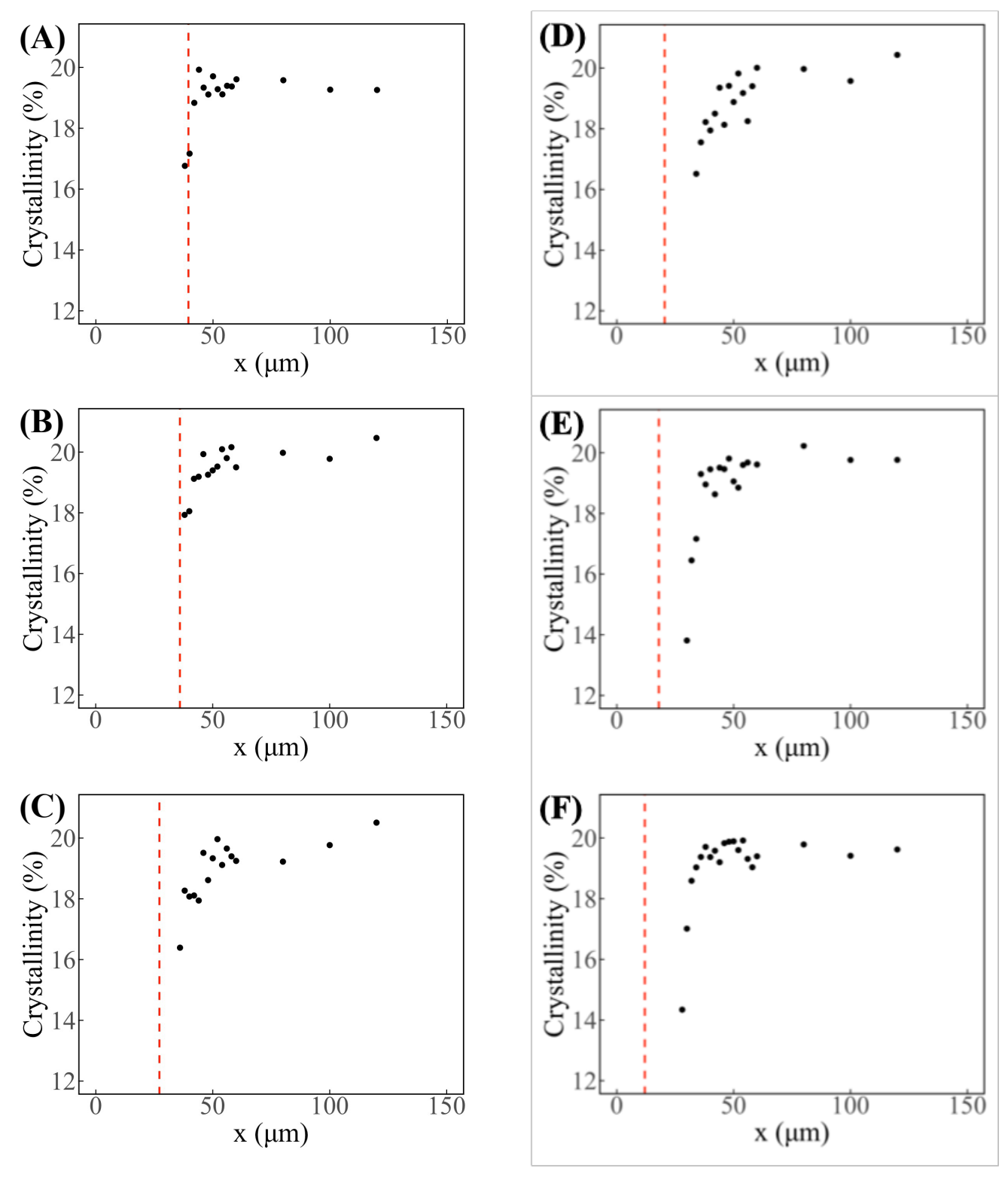


Fig. 5 The change in the degree of crystallinity as a function of measurement position under the following irradiation conditions: (A) 4.0 J/cm², 0.3 ps; (B) 4.0 J/cm², 1.2 ps; (C) 4.0 J/cm², 3.4 ps; (D) 4.0 J/cm², 7.6 ps; (E) 4.0 J/cm², 10 ps; (F) 3.4 J/cm², 10 ps. Dotted lines indicate the threshold for processing for each irradiation condition.

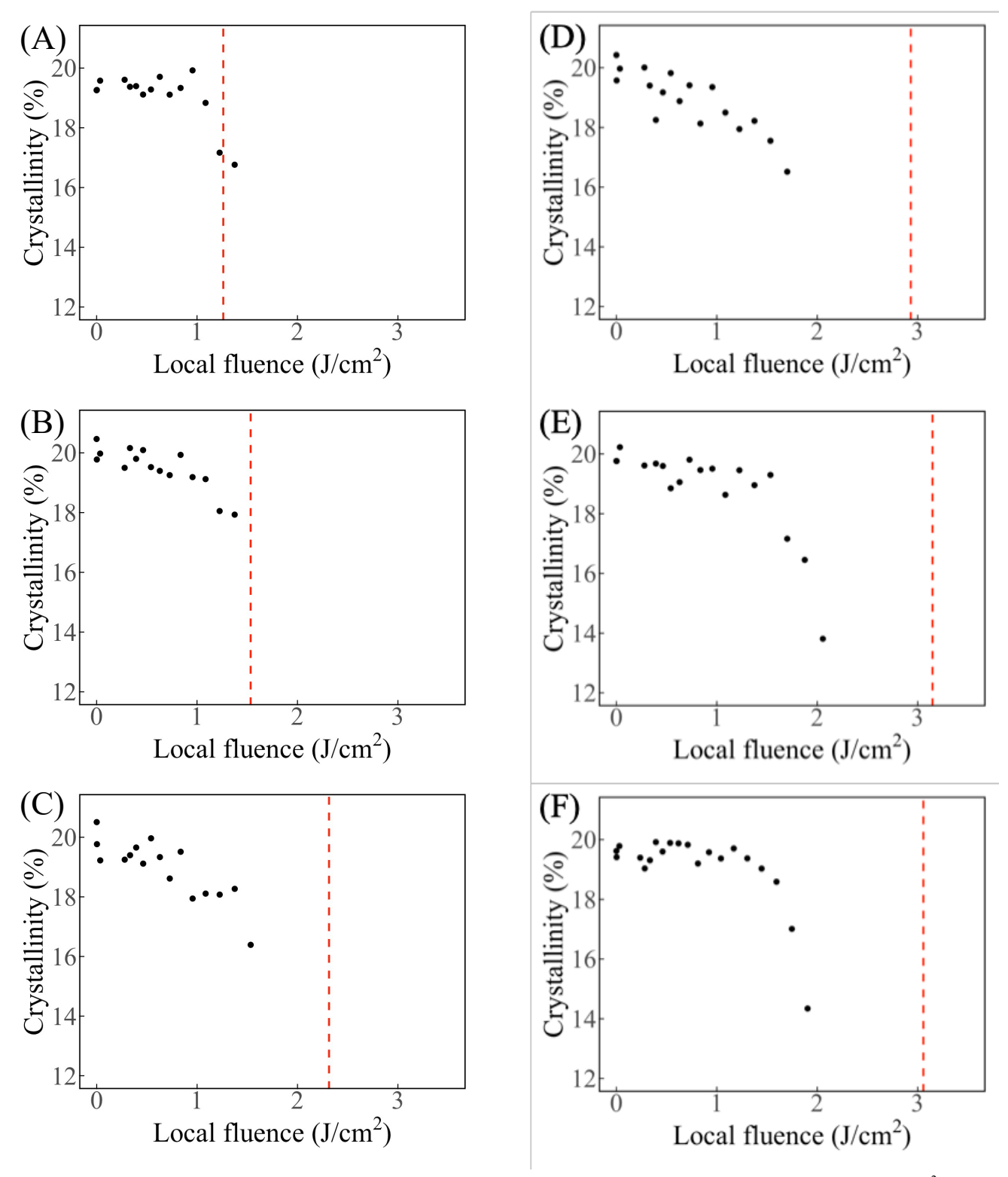


Fig. 6 Change in the degree of crystallinity as a function of local fluence under the following irradiation conditions: (A) 4.0 J/cm², 0.3 ps; (B) 4.0 J/cm², 1.2 ps; (C) 4.0 J/cm², 3.4 ps; (D) 4.0 J/cm², 7.6 ps; (E) 4.0 J/cm², 10 ps; (F) 3.4 J/cm², 10 ps. Dotted lines indicate the threshold fluence for processing for each irradiation condition.

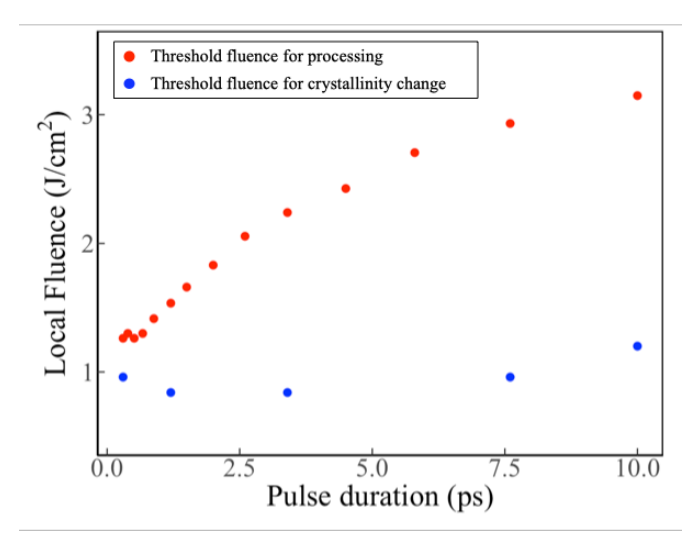


Fig. 7 The comparison between the threshold fluence for processing and the threshold fluence for crystallinity change. The red points indicate the threshold fluence for processing from 0.3 ps to 10 ps, while the blue points represent the fluence for crystallinity change, as shown in Figures 6 (A)–(E).

4. Conclusions

In this study, ultrashort pulse laser irradiation was applied to a 150 μm -thick PEEK film using single-shot pulses at a wavelength of 1.03 μm . The pulse duration was varied from 0.3 ps to 10 ps, and the peak fluence ranged from 0.2 to 4 J/cm². To evaluate changes in crystallinity around the irradiated crater, line-scan measurements were performed using micro-Raman spectroscopy at a wavelength of 1064 nm, with the center of the laser-irradiated spot defined as 0 μm . It was observed that, under the same fluence, the size of the laser-irradiated crater decreased as the pulse duration increased.

Under all irradiation conditions, the crystallinity decreased as the measurement position approached the laser-irradiated crater, indicating that changes in crystallinity occurred even outside the visibly irradiated area.

By converting the Raman measurement positions to local fluence for each condition, it was found that the threshold fluence for processing increased with increasing pulse duration, whereas the threshold fluence for crystallinity change remained nearly constant at approximately 1 J/cm².

These findings suggest that the threshold fluence for crystallinity change remains nearly constant, and consequently, that the region exhibiting crystallinity change does not significantly vary with increasing pulse duration.

Acknowledgments and Appendixes

This work was supported by JSPS KAKENHI, Grant Numbers JP23H01310 and JP23K26005. This work was conducted under the Visiting Researcher's Program of the Institute for Solid State Physics, University of Tokyo(IS-SPkyodo-202312-GNBXX-0030).

References

- [1] B. Pidhatika, V. T. Widyaya, P. C. Nalam, Y. A. Swasona, and R. Ardhani: Polym., 14, (2022) 5526.
- [2] A. Haleem and M. Javaid: Clin. Epidemiol. Glob. Health, 7, (2019) 571.

- [3] Q. Li, W. Perrie, Y. Tang, O. Allegre, J. Ho, P. Chalker, and Z. Li, S. Edwardson, and G. Dearden: Procedia CIRP, 94, (2020) 840.
- [4] S. Hammouti, B. Beaugiraud, M. Salvia, C. Mauclair, A. Pascale-Hamri, S. Benayoun, and S. Valette: Appl. Surf. Sci., 327, (2015) 277.
- [5] A. Sharif, N. Farid, Y. Liu, M. Wang, R. G. Palgrave, and G. M. O'Connor: Appl. Surf. Sci. Adv., 26, (2025) 100697.
- [6] J. Chen, Y. Li, M. Huang, and L. Dong: Int. J. Adhes. Adhes., 126, (2023) 103483.
- [7] B. Henriques, D. Fabris, B. Voisiat, and A. F. Lasagni: Mater. Lett., 339, (2023) 134091.
- [8] M. Regis, A. Bellare, T. Pascolini, and P. Bracco: Polym. Degrad. Stab., 136, (2017) 121.
- [9] T. J. Hoskins, K. D. Dearn, Y. K. Chen, and S. N. Kukureka: Wear, 309, (2014) 35.
- [10] D, Gaitanelis, A. Chanteli, C. Worrall, P. M. Weaver, and M. Kazilas: Polym. Degrad. Stab., 211, (2023) 110282.
- [11] A. Hartwig, J. Hunnekuhl, G. Vitr, S. Dieckhoff, F. Vohwinkel, and O. D. Hennemann: J. Appl. Polym. Sci., 64, (1997) 1091.
- [12] P. Laurens, B. Sadras, F. Decobert, F. Arefi-Khosari, and J. Amourousx: Int. J. Adhes. Adhes., 18, (1998)
- [13] M. Yamaguchi, S. Kobayashi, T. Numata, N. Kamihara, T. Shimada, M. Jikei, M. Muraoka, Jonathan. E. Barns ley, Sara. J. Fraser, Miller, and Keith. C. Gordon: J. Appl. Polym. Sci., 139(8), (2022) e51677.
- [14] E. Terasawa, T. Shibuya, D. Satoh, Y. Moriai, H. Ogawa, M. Tanaka, R. Kuroda, Y. Kobayashi, K. Sakaue, and M. Washio: Appl. Phys. A, 126, (2020) 446.
- [15] P. Wang, H. Yu, R. Ma, Y. Wang, C. Liu, and C. Shen: J. Therm. Anal. Calorim., 141, (2020) 1361.

(Received: June 30, 2025, Accepted: October 10, 2025)